

4. Y. Kamei *et al.*, *Cell* **85**, 403 (1997); D. Chakravarti *et al.*, *Nature* **383**, 99 (1996); H. Kawasaki *et al.*, *ibid.* **393**, 284 (1998).

5. P. H. Stern, in *Vitamin D*, D. Feldman, F. H. Glorieux, J. W. Pike, Eds. (Academic Press, New York, 1997), pp. 343–345; A. Takeshita *et al.*, *J. Biol. Chem.* **273**, 14738 (1998).

6. T. Yoshizawa *et al.*, *Nature Genet.* **16**, 391 (1997).

7. S. Kato *et al.*, *Science* **270**, 1491 (1995); K. Takeyama *et al.*, *ibid.* **277**, 1827 (1997).

8. K. Ebihara *et al.*, *Mol. Cell. Biol.* **16**, 3393 (1996).

9. S. Kato *et al.*, *ibid.* **15**, 5858 (1995).

10. COS-1 cells were maintained in Dulbecco's modified Eagle's medium without phenol red, supplemented with fetal bovine serum (5%) treated with dextran-coated charcoal. The cells were transfected at 40 to 50% confluency in 10-cm petri dishes with a total of 20 μ g of the indicated plasmids using calcium phosphate. All assays were done in the presence of 3 μ g of pCH110 (Pharmacia), a β -galactosidase expression vector, as an internal control to normalize for variations in transfection efficiency. Cognate ligands were added to the medium 1 hour after transfection and at each exchange of medium. After 24-hour incubation with the calcium phosphate-precipitated DNA, the cells were washed with fresh medium and incubated for an additional 24 hours. Cell extracts were prepared by freezing and thawing and were assayed for CAT activity after normalization for β -galactosidase activity as described (9).

11. The mammalian expression vector pCDNA3 (Invitrogen) was used for the expressions of Smad and SRC-1 proteins. Constitutively active and catalytically inactive forms of T β R-I, BMPR-IA, and BMPR-IB were as described (12). Full-length VDR and VDR mutants were inserted into the mammalian expression vector pSG5 (pSG5-VDR). DEF domains of VDR were inserted into the pM vector (Clontech) [GAL4-VDR(DEF)] and full-length Smad2 and Smad3 were inserted into pVP (Clontech) (VP16-Smad2 and VP16-Smad3).

12. T. Imamura *et al.*, *Nature* **389**, 622 (1997).

13. J. Yanagisawa *et al.*, unpublished data.

14. J. Massague, *Cell* **85**, 947 (1996); C.-H. Heldin, K. Miyazono, P. ten Dijke, *Nature* **390**, 465 (1997); J. R. Howe *et al.*, *Science* **280**, 1086 (1998).

15. M. Kretschmar *et al.*, *Genes Dev.* **11**, 984 (1997); A. Suzuki *et al.*, *Dev. Biol.* **184**, 402 (1997); J. M. Graff, A. Bansal, D. A. Melton, *Cell* **85**, 479 (1996).

16. P. A. Hoodless *et al.*, *Cell* **85**, 489 (1996); F. Liu *et al.*, *Nature* **381**, 620 (1996).

17. M. Macias-Silva *et al.*, *Cell* **87**, 1215 (1996); A. Nakao *et al.*, *EMBO J.* **16**, 5353 (1997); J. C. Baker and R. M. Harland, *Genes Dev.* **10**, 1880 (1996).

18. G. Lagna *et al.*, *Nature* **383**, 832 (1996); Y. Zhang *et al.*, *ibid.*, p. 168.

19. X. Chen, M. J. Rubock, M. Whitman, *ibid.*, p. 691; J. Kim *et al.*, *ibid.* **388**, 304 (1997); S. Dennler *et al.*, *EMBO J.* **17**, 3091 (1998); L. Zawel *et al.*, *Mol. Cell* **1**, 611 (1998).

20. Y. Zhang, T. Musci, R. Derynck, *Curr. Biol.* **7**, 270 (1997).

21. GAL4 DNA-binding domain fusions were generated in pM, and VP16 fusions within pVP16. Interactions were tested in COS-1 cells. Activation of the CAT reporter-bearing GAL4-binding elements (17Mx5) was assayed in the presence or absence of 1,25(OH)₂D₃.

22. COS-1 cells were transfected with the indicated plasmids, lysed in TNE buffer [10 mM Tris-HCl (pH 7.8), 1% NP-40, 0.15 M NaCl, 1 mM EDTA], and immunoprecipitated with monoclonal antibody to FLAG (IBI; Eastman Kodak). Interacting proteins were separated by 8% SDS-polyacrylamide gel electrophoresis (SDS-PAGE), transferred onto polyvinylidene difluoride membranes (Bio-Rad), and then detected with antibody to VDR and antibody to rabbit immunoglobulin G conjugated with alkaline phosphatase (Promega).

23. GST-fused proteins were expressed in *Escherichia coli* and purified on glutathione-Sepharose beads (Pharmacia). The beads were incubated with [³⁵S]methionine-labeled proteins. Bound proteins were eluted and analyzed by SDS-PAGE.

24. Proteins were translated in vitro in the presence of [³⁵S]methionine with the reticulocyte lysate system (Promega).

25. D. M. Heery *et al.*, *Nature* **387**, 733 (1997); H.

Masuyama *et al.*, *Mol. Endocrinol.* **11**, 1507 (1997); C. H. Jin *et al.*, *ibid.* **10**, 945 (1996).

26. Cells were harvested and washed twice with ice-cold phosphate-buffered saline. Centrifuged cells were resuspended in 4 ml ice-cold lysis buffer [10 mM Tris-HCl (pH 7.4), 10 mM NaCl, 3 mM MgCl₂, 0.5% (v/v) NP-40] and incubated on ice for 15 min, then centrifuged again for 5 min at 500g. The sedimented nuclear fraction was resuspended in TNE buffer [10 mM Tris-HCl (pH 7.8), 1% NP-40, 0.15 M NaCl, 1 mM EDTA], incubated for 30 min on ice, and centrifuged. The supernatant was used as nuclear extract for the experiments.

27. T. Spencer *et al.*, *Nature* **389**, 194 (1997); T. Yao *et al.*, *Proc. Natl. Acad. Sci. U.S.A.* **93**, 10626 (1997).

28. J. J. Voegel *et al.*, *EMBO J.* **17**, 507 (1998).

29. Single-letter abbreviations for the amino acid residues are as follows: A, Ala; C, Cys; D, Asp; E, Glu; F, Phe; G, Gly; H, His; I, Ile; K, Lys; L, Leu; M, Met; N, Asn; P, Pro; Q, Gln; R, Arg; S, Ser; T, Thr; V, Val; W, Trp; and Y, Tyr. X indicates any residue.

30. We thank P. Chambon for critical reading of the manuscript and for providing nuclear receptor expression vectors, H. Gronemeyer for providing TIF2 expression vectors, R. H. Goodman for the CBP cDNA, and S. Hanazawa and A. Takeshita for helpful discussion.

23 June 1998; accepted 22 January 1999

p53- and ATM-Dependent Apoptosis Induced by Telomeres Lacking TRF2

Jan Karlseder,^{1*} Dominique Broccoli,^{1*†} Yumin Dai,² Stephen Hardy,^{2‡} Titia de Lange^{1§}

Although broken chromosomes can induce apoptosis, natural chromosome ends (telomeres) do not trigger this response. It is shown that this suppression of apoptosis involves the telomeric-repeat binding factor 2 (TRF2). Inhibition of TRF2 resulted in apoptosis in a subset of mammalian cell types. The response was mediated by p53 and the ATM (ataxia telangiectasia mutated) kinase, consistent with activation of a DNA damage checkpoint. Apoptosis was not due to rupture of dicentric chromosomes formed by end-to-end fusion, indicating that telomeres lacking TRF2 directly signal apoptosis, possibly because they resemble damaged DNA. Thus, in some cells, telomere shortening may signal cell death rather than senescence.

Mammalian telomeres consist of several kilobases of tandem TTAGGG repeats bound by the related telomere-specific proteins, TRF1 and TRF2 (1). TRF1 regulates telomere length (2) and TRF2 maintains telomere integrity (3). Inhibition of TRF2 results in loss of the G-strand overhangs from telomere termini and induces covalent fusion of chromosome ends (3, 4).

To investigate the cellular consequences of telomere malfunction, we used adenoviral vectors to overexpress intact and truncated versions of TRF1 and TRF2 (Fig. 1) (5). These vectors encoded full-length TRF1 (AdTRF1); a dominant negative version of TRF1 lacking the Myb DNA binding domain (AdTRF1^{ΔM}); full-length TRF2 (AdTRF2); an NH₂-terminal deletion of TRF2 lacking the TRF2-specific basic

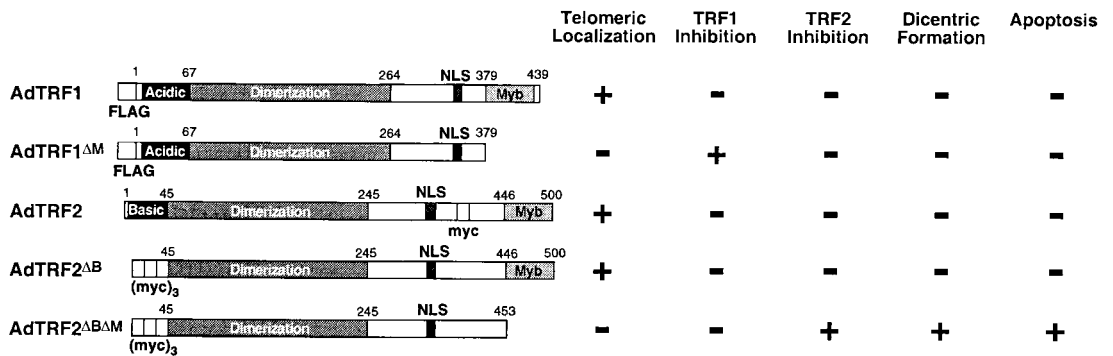
Table 1. Cell type dependence of AdTRF2^{ΔBΔM}-induced apoptosis.

Cell line/strain	Chromosome fusions per anaphase*		% cells undergoing apoptosis†	
	Uninfected	AdTRF2 ^{ΔBΔM}	Uninfected	AdTRF2 ^{ΔBΔM}
HeLa11 \ddagger (cervical carcinoma)	0.1 \pm 0.01	1.2 \pm 0.04	2.7 \pm 0.6	38 \pm 1.0
HeLa1.2.11 \ddagger (cervical carcinoma)	0.1 \pm 0.01	0.9 \pm 0.07	2.0 \pm 1.0	40 \pm 1.7
MCF7 (mammary adenocarcinoma)	0.1 \pm 0.01	0.9 \pm 0.06	3.0 \pm 1.0	29 \pm 1.2
CD4 ⁺ T cells	0.2 \pm 0.01	0.9 \pm 0.02	6.3 \pm 0.6	39 \pm 1.5
HT-1080 (fibrosarcoma)	0.1 \pm 0.01	0.9 \pm 0.03	1.0 \pm 0.1	1.3 \pm 0.6
Saos-2 (osteosarcoma)	<0.1	1.3 \pm 0.01	2.0 \pm 1.0	2.3 \pm 0.6
SW 626 (ovarian carcinoma)	<0.1	0.9 \pm 0.04	3.0 \pm 0.1	3.7 \pm 0.6
WI-38 (fetal lung fibroblasts)	<0.1	1.2 \pm 0.01	<0.01	<0.01
HS68 (foreskin fibroblasts)	<0.1	0.9 \pm 0.10	<0.01	<0.01
MRC-5 (fetal lung fibroblasts)	<0.1	0.9 \pm 0.08	<0.01	<0.01
IMR-90 (fetal lung fibroblasts)	<0.1	1.5 \pm 0.01	<0.01	<0.01

*Infected cells (72 hours) were stained with DAPI and anaphases were examined for evidence of chromosome fusions (chromatin bridges and lagging chromosomes). The numbers indicated average fusion events per anaphase from three independent experiments and the SD. SDs below 0.01 are given as 0.01. †Percentage of cells positive for TUNEL labeling 72 hours after infection. Apoptotic CD4⁺ T cells were counted 48 hours after infection. The numbers are averages from three independent experiments and the SD. SDs below 0.1 are given as 0.1. ‡HeLa11 and HeLa1.2.11 are HeLa subclones.

REPORTS

Fig. 1. Adenovirally expressed TRF1 and TRF2 proteins. Expression of the indicated TRF proteins was monitored by immunoblotting, and their localization was determined by IF (6). Inhibition of TRF1 and TRF2 was determined by gel-shift assay (9) and IF (3), respectively. Dicentric formation was deduced from the presence of anaphase bridges in infected cells.



domain (AdTRF2 Δ B); and a dominant negative version of TRF2 lacking both the basic domain and the Myb domain (AdTRF2 Δ B Δ M). Transformed and primary cells were infected efficiently, resulting in overexpression of the different TRF proteins at approximately the same levels (6).

Indirect immunofluorescence analysis (2, 3, 7) indicated that TRFs retaining the Myb domain localized to telomeres, as deduced from their characteristic punctate staining pattern in interphase nuclei (Fig. 1) (6). In contrast, TRFs lacking the Myb domain did not accumulate at telomeres but displayed a dispersed nuclear staining pattern. Expression of AdTRF1 Δ M reduced the TRF1-specific TTAGGG repeat binding activity in cell extracts (8, 9), implying that this allele has the expected dominant interfering effect on the DNA binding activity of endogenous TRF1. The dominant negative effect of AdTRF2 Δ B Δ M was documented based on displacement of the endogenous TRF2 protein from the telomeres and its ability to induce chromosome end fusions (Fig. 1 and Table 1) (3).

AdTRF2 Δ B Δ M resulted in a rapid induction of apoptosis in infected HeLa cells, as assessed by TUNEL labeling, Annexin-V staining, and the appearance of cells with a sub-G₁ DNA content in fluorescence activated cell sorting (FACS) analysis (10) (Fig. 2, A and B). HeLa cells transfected with an unrelated TRF2 Δ B Δ M expression construct lacking adenoviral sequences had the same response, demonstrating that apoptosis did not require adenoviral gene products. None of the other TRF alleles affected cell viability or growth in the short term, although a minor G₂ accumulation phenotype occurred in HeLa cells expressing

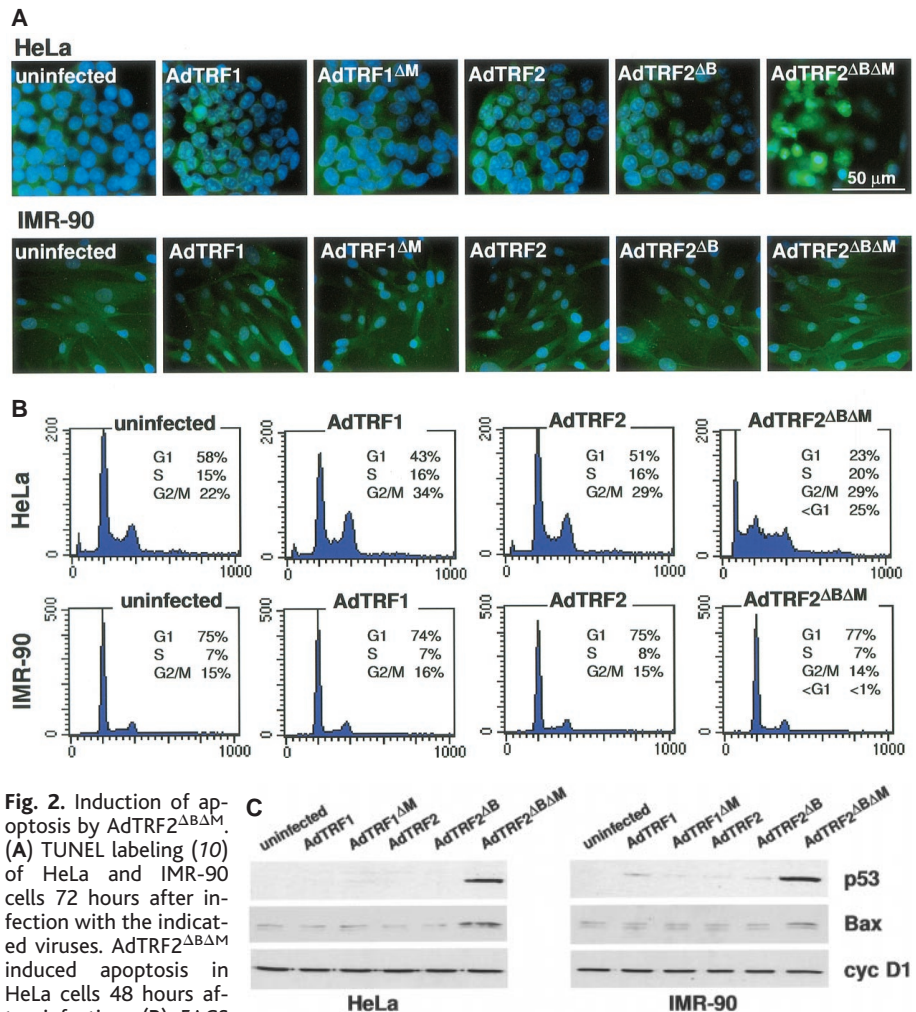


Fig. 2. Induction of apoptosis by AdTRF2 Δ B Δ M. (A) TUNEL labeling (10) of HeLa and IMR-90 cells 72 hours after infection with the indicated viruses. AdTRF2 Δ B Δ M induced apoptosis in HeLa cells 48 hours after infection. (B) FACS analysis (10) of HeLa and IMR-90 cells 72 hours after infection with the indicated adenoviruses. Y-axis: cell numbers; X-axis: relative DNA content, based on staining with propidium iodide. (C) Immunoblot analysis (15) of p53, Bax, and cyclin D1 (as a loading control) in HeLa and IMR-90 cells infected with the indicated adenoviruses.

full-length TRF1 and TRF2 (Fig. 2B) (11). The absence of apoptosis with AdTRF2 and AdTRF2 Δ B suggested that AdTRF2 Δ B Δ M induced apoptosis by reducing the amount of TRF2 bound to telomeres.

In contrast to HeLa cells, the HDF cell strain IMR-90 and the fibrosarcoma cell line HT-1080 did not undergo apoptosis after in-

hibition of TRF2 (Fig. 2A) (3). To explore the cell-type dependence of the apoptotic response, we infected several immortalized human cell lines and primary human cell strains with AdTRF2 Δ B Δ M. Apoptosis was observed in two HeLa subclones, the p16-deficient mammary adenocarcinoma cell line MCF7, immortalized B cells (see below), and prima-

¹Laboratory for Cell Biology and Genetics, The Rockefeller University, New York, NY 10021, USA. ²Cell Genesys, Foster City, CA 94405, USA.

*These authors contributed equally to this work.
†Present address: Fox Chase Cancer Center, 7701 Burholme Avenue, Philadelphia, PA 19111, USA.
‡Present address: Chiron Corporation, 4560 Horton Street, Mailstop 4-3, Emeryville, CA 94608-2916, USA.

§To whom correspondence should be addressed. E-mail: delange@rockvax.rockefeller.edu

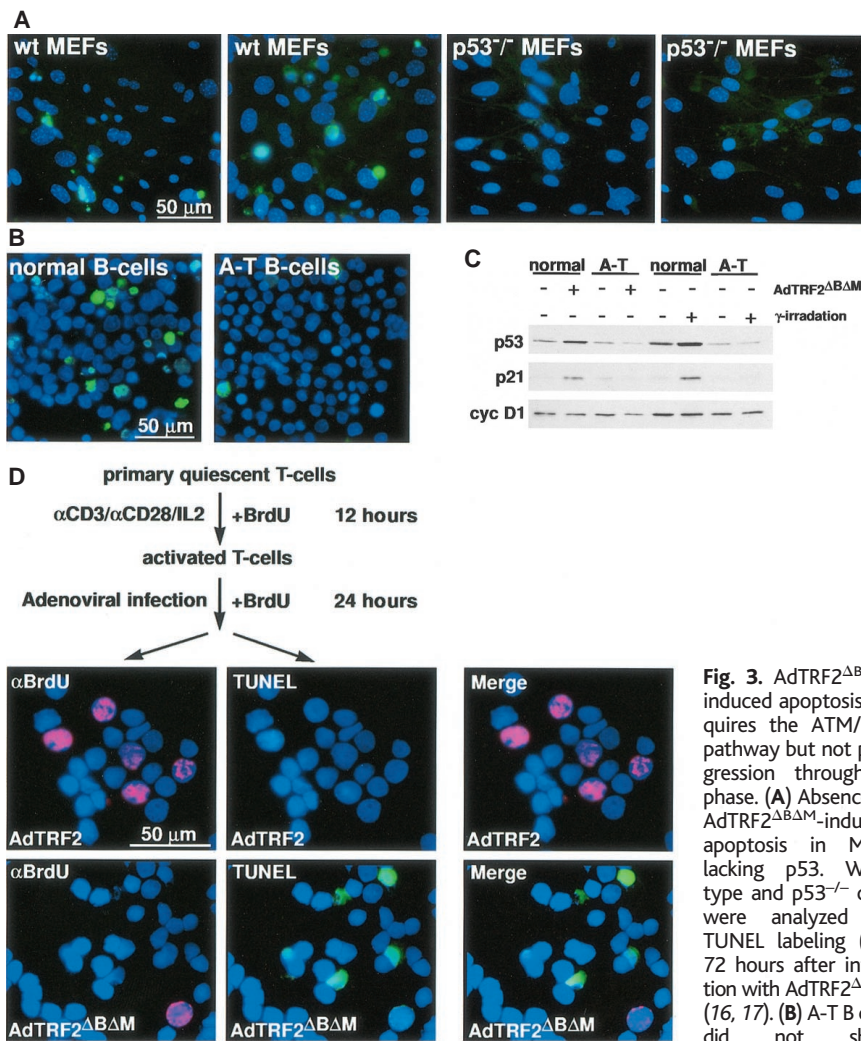


Fig. 3. AdTRF2^{ΔBΔM}-induced apoptosis requires the ATM/p53 pathway but not progression through S phase. (A) Absence of AdTRF2^{ΔBΔM}-induced apoptosis in MEFs lacking p53. Wild-type and p53^{-/-} cells were analyzed by TUNEL labeling (10) 72 hours after infection with AdTRF2^{ΔBΔM} (16, 17). (B) A-T B cells did not show AdTRF2^{ΔBΔM}-induced

apoptosis. Human B cell lines from a normal donor (GM130C) and an A-T patient (GM01526E) expressing AdTRF2^{ΔBΔM} were analyzed for apoptosis by TUNEL labeling (10) at 24 hours after infection. (C) Immunoblot (15) of p53, p21, and cyclin D1 levels in B cells derived from normal and A-T donors 20 hours after infection with the indicated adenoviruses or γ-irradiation. (D) Progression through S phase is not required for the induction of apoptosis. Top, schematic of the experiment. Bottom, detection of BrdU uptake and TUNEL labeling in T cells infected with the indicated adenoviruses (24).

ry CD4⁺ T cells (Table 1). Cells that failed to undergo apoptosis in response to AdTRF2^{ΔBΔM} either lacked an apoptotic response to DNA damage (12) or were deficient for p53 function (13). Although HeLa cells are partially compromised for p53 function because they express human papilloma virus-16 E6 tumor antigen, which targets p53 for degradation, they do contain a fully functional p53 pathway (14). To investigate this pathway, we examined protein levels of p53 and its downstream target Bax in HeLa cells expressing the five different TRF alleles (15). p53 levels rose only in response to AdTRF2^{ΔBΔM} and there was a concomitant increase in the expression of Bax (Fig. 2C), indicating that p53 is activated as a transcription factor. Induction of p53 and Bax was also observed in cells not undergoing apoptosis.

The role of p53 was confirmed using mouse embryo fibroblasts (MEFs) from genetically al-

tered mice. The dimerization domains of human TRF2 and mouse Trf2 are nearly identical (1), suggesting that the mouse protein would be inhibited by AdTRF2. Indeed, wild-type MEFs infected with AdTRF2^{ΔBΔM} lost the punctate nuclear pattern typical of Trf2 engaged on telomeres and showed chromosome end fusions (Table 2), validating the use of AdTRF2^{ΔBΔM} in murine cells (16, 17). Wild-type MEFs and MEFs from p21 (18), INK4a/ARF (19), or RB (20) knockout mice showed a strong apoptotic response to AdTRF2^{ΔBΔM} (~18% apoptosis) (Fig. 3A and Table 2), while uninfected controls and cells infected with AdTRF2 or AdTRF2^{ΔB} showed background levels of apoptosis [2 to 5%; (Table 2) (17)]. In contrast, MEFs derived from p53^{-/-} mice (21) did not show this apoptotic response (Fig. 3A and Table 2). The AdTRF2^{ΔBΔM} protein was clearly active as a dominant negative allele in the

p53^{-/-} MEFs, since the cells displayed a high rate of anaphase bridge formation. These data establish a requirement for p53 function in the telomere-mediated apoptotic pathway.

p53 can be phosphorylated by the ATM kinase, the product of the gene that is mutated in patients with ataxia-telangiectasia (A-T) (22). ATM is thought to function upstream of p53 in a DNA damage response pathway because A-T cells show diminished induction of p53 and reduced ability to arrest in G₁ after ionizing radiation (23). To explore the possibility that ATM also functions in the telomere-directed apoptotic response documented here, we analyzed the effect of AdTRF2^{ΔBΔM} on the viability of human B cell lines from A-T patients and normal donors. Normal B cell lines rapidly underwent apoptosis, whereas B cells from A-T patients did not show this response (Fig. 3B and Table 2). In addition, paralleling their response to γ-irradiation, B cells from A-T patients showed no evidence of p53 induction or up-regulation of the p53 target p21 after infection with AdTRF2^{ΔBΔM} (Fig. 3C). Thus, similar to the signaling pathway activated by double-stranded breaks, the induction of apoptosis by telomere malfunction requires ATM, most likely as an upstream activator of p53.

Two types of events might be responsible for the activation of the ATM/p53-dependent apoptotic pathway. Because loss of TRF2 function induces covalent fusion of telomeres (3, 4), mitotic rupture of dicentric chromosomes will generate DNA breaks that can activate a DNA damage response. However, a signal could also emanate directly from the chromosome ends, if telomeres lacking TRF2 resemble damaged DNA. To distinguish between these possibilities, we determined whether progression through mitosis is required for the AdTRF2^{ΔBΔM}-induced apoptosis. Primary human peripheral T cells were harvested in a quiescent state, stimulated to proliferate in the presence of bromodeoxyuridine (BrdU), and infected with AdTRF2^{ΔBΔM} and AdTRF2 prior to entry into S phase (24). Cells were simultaneously examined for BrdU incorporation and apoptosis 24 hours later (Fig. 3D). Although adenovirus infection inhibited T cell proliferation slightly, a substantial fraction of the cells progressed through S phase and incorporated BrdU. As expected, AdTRF2^{ΔBΔM}, but not AdTRF2, induced apoptosis in primary T cells. While some cells showed dual labeling for both BrdU and TUNEL, a substantial proportion (~80%) of the apoptotic cells in the AdTRF2^{ΔBΔM}-infected cultures did not contain detectable amounts of BrdU (Fig. 3D). Thus, a subset of the AdTRF2^{ΔBΔM}-infected cells entered apoptosis before progressing through S-phase, and hence before undergoing mitosis. This interpretation is corroborated by the drop in BrdU-positive cells in AdTRF2^{ΔBΔM}-infected T cells (Fig. 3D) (24). Based on these data, we conclude

REPORTS

Table 2. Requirement of p53 and ATM for AdTRF2^{ΔBΔM}-induced apoptosis.

Cell strain/ genotype	Chromosome fusions per anaphase*		% cells undergoing apoptosis*	
	uninfected	AdTRF2 ^{ΔBΔM}	uninfected	AdTRF2 ^{ΔBΔM}
		<i>MEFs</i>		
Wild-type	0.3 ± 0.11	0.9 ± 0.07	5.0 ± 1.7	18 ± 1.0
pRb-/-	0.1 ± 0.05	0.8 ± 0.13	4.0 ± 0.1	19 ± 2.0
INK4a/ARF-/-	0.1 ± 0.04	0.7 ± 0.12	3.7 ± 1.2	19 ± 4.0
p21-/-	0.1 ± 0.07	0.8 ± 0.07	5.3 ± 1.2	19 ± 1.7
p53-/-	0.1 ± 0.07	0.8 ± 0.18	3.7 ± 1.5	3.7 ± 0.6
		<i>B cells</i> †		
GM130C normal	0.2 ± 0.04	0.9 ± 0.12	8.0 ± 0.1	53 ± 0.1
GM13068 normal	0.1 ± 0.12	1.0 ± 0.01	8.0 ± 1.4	45 ± 4.9
GM01526E A-T	0.1 ± 0.15	0.9 ± 0.23	8.5 ± 0.7	12 ± 0.7
GM8436A A-T	0.2 ± 0.03	0.8 ± 0.06	6.0 ± 1.4	7 ± 0.1

*See Table 1. MEFs and B cells were analyzed 96 and 24 hours after infection, respectively. †Normal and A-T B cells were obtained from the NIGMS Human Genetic Mutant Cell Repository.

that in primary human T cells, inhibition of TRF2 function can induce apoptosis independent of the damage resulting from broken dicentric chromosomes.

Collectively, these data reveal a previously unrecognized function of mammalian telomeres: their ability to prevent the induction of apoptosis by chromosome ends. We considered the possibility that inhibition of TRF2 might result in sudden loss of telomeric DNA, leaving uncapped chromosome ends that could activate a DNA damage checkpoint. However, HeLa and IMR-90 cells infected with AdTRF2^{ΔBΔM} showed no loss of TTAGGG repeat DNA detectable by standard genomic blotting. Thus, binding of TRF2 to the TTAGGG repeats is apparently required to “mask” chromosome ends from a response pathway that can lead to cell death. The exact nature of the apoptotic signal from the unmasked telomeres remains to be established. The involvement of ATM suggests that inappropriately exposed telomeric DNA might resemble a double-stranded break, which is the predominant initiating signal for ATM-mediated p53 activation [reviewed in (25)]. Cells expressing TRF2^{ΔBΔM} rapidly lose the 3' overhang of telomeric TTAGGG repeats that protrudes from human telomeres (3), so conceivably, this unique feature of telomeres may be a criterion by which random double-stranded breaks are distinguished from natural chromosome ends. However, we cannot exclude the existence of an ATM/p53-dependent telomeric checkpoint that directly senses the altered status of the telomeric complex in TRF2^{ΔBΔM}-expressing cells.

Compromised telomere function leads to deregulation of telomere length, fusions of chromosome ends, and senescence (2, 3, 26). Our data indicate that at least in some mammalian cell types, telomere malfunction can also induce apoptosis, a suggestion consistent with the increased rate of apoptosis in mice with critically shortened telomeres (27). Thus, disintegration of the telomeric complex as a con-

sequence of telomere erosion in the human soma may cause apoptosis of some cells (such as T cells) and senescence of others (such as fibroblasts). Since telomeres also shorten during tumorigenesis (28), induction of the apoptotic pathway described here may provide an additional selection for malignant cells that are deficient in p53 function.

References and Notes

1. L. Chong *et al.*, *Science* **270**, 1663 (1995); D. Broccoli *et al.*, *Nature Genet.* **17**, 231 (1997); T. Bilaud *et al.*, *ibid.*, p. 236.
2. B. van Steensel and T. de Lange, *Nature* **385**, 740 (1997).
3. B. van Steensel, A. Smogorzewska, T. de Lange, *Cell* **92**, 401 (1998).
4. A. Smogorzewska and T. de Lange, unpublished observations.
5. S. Hardy *et al.*, *J. Virol.* **71**, 1842 (1997).
6. Details of the cloning of the adenoviral constructs and the expression of the TRF alleles are given at the *Science* Web site (www.sciencemag.org/feature/data/986472.shl). Plaque-purified viruses were expanded on 293 cells, purified by CsCl banding, and stored at -20°C in 50% glycerol. For infections, 2 × 10⁵ cells were mixed with virus in 1.4 ml of media and plated into six-well dishes. HeLa, Saos-2, SW 626, and HT-1080 were infected with 12 plaque-forming units (pfu) per cell; IMR-90, WI-38, HS68, and MRC-5 with 36 pfu/cell; MEFs with 100 pfu/cell; and B and T cells with 360 pfu/cell. We have found that long-term (>4 days) adenovirus infection inhibits cell growth and alters the expression of cell-cycle markers. For this reason, data were collected within 96 hours after infection. The adenoviral growth inhibition prevented the analysis of a possible senescence response to TRF proteins.
7. We used the M2 monoclonal antibody (Kodak) to detect the FLAG epitope, the 9E10 monoclonal antibody to detect the myc tag, antibody #371 to detect TRF1 and antibody #508 to detect TRF2 by indirect immunofluorescence (IF) (2, 3). Rabbit antibodies (#371 and #508) were detected with tetramethyl rhodamine isothiocyanate (TRITC)-conjugated donkey antibodies to rabbit immunoglobulin (IgG), and mouse antibodies (M2, 9E10) were detected with fluorescein isothiocyanate (FITC)-conjugated donkey antibodies to mouse IgG (Jackson). The secondary antibodies did not cross-react. DNA was stained with 4,6-diamino-2-phenylindole (DAPI) (0.2 μg/ml).
8. A. Bianchi *et al.*, *EMBO J.* **16**, 1785 (1997).
9. TRF1 gel-shift assays (8) were performed with 2 μg cellular protein extracted in buffer containing 0.1% NP-40 and 0.4 M KCl (2) at 48 hours after infection. A 90% drop in TRF1 binding activity was observed in

extracts of cells expressing AdTRF1^{ΔM} as compared to noninfected control cells.

10. TUNEL labeling was performed using the Oncor ApoTag Direct In Situ Apoptosis Detection Kit. Annexin-V labeling was performed using a Clontech ApoAlert Annexin-V-FITC Apoptosis kit. For FACS analysis, 2 × 10⁵ cells were fixed in 70% ethanol, stained with propidium iodide, and analyzed using a Becton-Dickinson FACSscan and CellQuest software.
11. M. Shen *et al.*, *Proc. Natl. Acad. Sci. U.S.A.* **94**, 13618 (1997). The modest G₂ accumulation observed in HeLa cells infected with AdTRF1 and AdTRF2 appears to be a HeLa-specific phenotype because it does not occur in HT-1080 (2), WI-38, and IMR-90.
12. A. Di Leonardo *et al.*, *Genes Dev.* **8**, 2540 (1994); J. Yeargin and M. Haas, *Curr. Biol.* **5**, 423 (1995).
13. X. Chen, L. J. Ko, L. Jayaraman, C. Prives, *Genes Dev.* **10**, 2438, (1996); T. Strobel *et al.*, *Proc. Natl. Acad. Sci. U.S.A.* **93**, 14094 (1996).
14. M. Scheffner *et al.*, *Cell* **63**, 1129 (1990).
15. Protein (30 μg) extracted in 50 mM Hepes-KaOH (pH 7.5), 150 mM NaCl, 1 mM EDTA, 2.5 mM EGTA, and 0.5% NP-40 was fractionated on SDS-polyacrylamide gels, transferred to nitrocellulose membranes, blocked in phosphate-buffered saline (PBS) containing 10% milk and 0.1% Tween 20, and incubated in PBS with 0.1% milk and 0.1% Tween 20 with the following antibodies: anti-p53 (Santa Cruz DO1), anti-Cyclin D1 (Santa Cruz R124), anti-Bax (Santa Cruz B-9), anti-p21 (Santa Cruz F-5), anti-FLAG (Kodak M2), or anti-myc 9E10. Blots were washed (three times) in PBS with 0.1% milk and 0.1% Tween 20 and incubated with horseradish peroxidase-conjugated donkey anti-rabbit or sheep anti-mouse (Amersham). Bound antibodies were detected using the ECL kit (Amersham).
16. MEFs (passage 6 or less) were grown in Dulbecco's modification of Eagle's medium and 15% fetal bovine serum. Although MEFs show diminished infectability with adenoviruses, satisfactory infection levels (90%) can be achieved using a threefold higher multiplicity of infection compared to primary human fibroblasts (100 pfu/cell). Although MEFs normally do not undergo apoptosis in response to DNA damage, when infected with adenovirus, they display a strong apoptotic response 72 hours after γ-irradiation (20 gray). Thus, the apoptotic response of MEFs to AdTRF2^{ΔBΔM} is partly due to adenoviral infection. However, adenoviral infection alone does not initiate an apoptotic response, because MEFs infected with AdTRF2 or AdTRF2^{ΔB} did not show more TUNEL-positive cells 96 hours after infection than did uninfected controls.
17. To document the dominant negative activity of AdTRF2^{ΔBΔM} in MEFs, we stained cells with anti-hTRF2 #508 (3), which cross-reacts with mouse Trf2, generating a punctate nuclear pattern, reflecting TRF2 on mouse telomeres. Upon infection of MEFs with AdTRF2^{ΔBΔM}, this punctate pattern was lost or reduced (3). The dominant negative activity of AdTRF2^{ΔBΔM} was also evident from the induction of anaphase bridges and apoptosis.
18. C. Deng *et al.*, *Cell* **82**, 675 (1995).
19. M. Serrano *et al.*, *ibid.* **85**, 27 (1996).
20. E. H. Lee *et al.*, *Nature* **359**, 288 (1992).
21. T. Jacks *et al.*, *Curr. Biol.* **4**, 1 (1994).
22. S. Banin *et al.*, *Science* **281**, 1674 (1998); C. E. Canman *et al.*, *ibid.*, p. 1677.
23. M. B. Kastan *et al.*, *Cell* **71**, 587 (1992); Y. Xu and D. Baltimore, *Genes Dev.* **10**, 2401 (1996); X. Lu and D. P. Lane, *Cell* **75**, 765 (1993).
24. CD4⁺ T cells were isolated using a MiniMACS column and αCD4 beads, as described by the supplier (Milteny Biotech). Alternatively, primary human T cells were purified by a modification (www.sciencemag.org/feature/data/986472.shl) of a previously described method [D. Unutmaz, P. Pileri, S. Abrignani, *J. Exp. Med.* **180**, 1159 (1994)]. Resting T cells (99%) were enriched using depletion with antibodies to HLA-DR [American Type Culture Collection (ATCC)] and CD69 (Pharmingen) adsorbed onto Dynabeads (Dyna). T cells were stimulated with anti-CD3 (OKT-3; ATCC) and anti-CD28 (Pharmingen) in RPMI medium containing recombinant human interleukin-2 (200 U/ml) and 1 μM

BrdU. After 12 hours, cells were infected with adenoviruses in fresh medium containing 1 μ M BrdU. Cells were collected onto cover slips at 24 hours after infection, fixed for 1 hour at -20°C in 70% ethanol and 50 mM glycine (pH 2.5), and processed for TUNEL labeling. Subsequently, BrdU incorporation was visualized with a Boehringer BrdU Labeling and Detection Kit #1 with a TRITC-coupled secondary antibody (Jackson). Based on the BrdU incorporation, infection with AdTRF2 and AdTRF2 Δ BM resulted in 55% and 83% inhibition of S phase, respectively.

25. M. F. Lavin and Y. Shiloh, *Annu. Rev. Immunol.* **15**, 177 (1997).
26. A. G. Bodnar *et al.*, *Science* **279**, 349 (1998); H. Vaziri and S. Benchimol, *Curr. Biol.* **8**, 279 (1998); J. Wang, *et al.*, *Genes Dev.* **12**, 1769 (1998); T. de Lange, *Science* **279**, 334 (1998); C. W. Greider, *Curr. Biol.* **8**, R178 (1998).
27. H. W. Lee *et al.*, *Nature* **392**, 569 (1998).
28. T. de Lange *et al.*, *Mol. Cell. Biol.* **10**, 518 (1990); N. Hastie *et al.*, *Nature* **346**, 866 (1990).
29. We thank T. Jacks and R. DePinho for MEFs and

helpful discussion; N. Dyson, C. Sherr, C. Prives, and K. Kuchler for antibodies; D. Unutmaz and M. Alberts for primary human T cells; T. Jenuwein for CMV-myc TRF1; F. Isdell for expert assistance in the FACS analysis; and C. Price and members of the de Lange lab for their insights. Supported by the Human Frontiers Science Program (J.K.), Merck (D.B.), and grants from the New York Community Trust, Rita Allen Foundation, and NIH (GM49046) (T.d.L.).

12 November 1998; accepted 26 January 1999

Function of WW Domains as Phosphoserine- or Phosphothreonine-Binding Modules

Pei-Jung Lu,* Xiao Zhen Zhou,* Minhui Shen, Kun Ping Lu†

Protein-interacting modules help determine the specificity of signal transduction events, and protein phosphorylation can modulate the assembly of such modules into specific signaling complexes. Although phosphotyrosine-binding modules have been well-characterized, phosphoserine- or phosphothreonine-binding modules have not been described. WW domains are small protein modules found in various proteins that participate in cell signaling or regulation. WW domains of the essential mitotic prolyl isomerase Pin1 and the ubiquitin ligase Nedd4 bound to phosphoproteins, including physiological substrates of enzymes, in a phosphorylation-dependent manner. The Pin1 WW domain functioned as a phosphoserine- or phosphothreonine-binding module, with properties similar to those of SRC homology 2 domains. Phosphoserine- or phosphothreonine-binding activity was required for Pin1 to interact with its substrates *in vitro* and to perform its essential function *in vivo*.

Interactions through specific protein modules help determine the specificity of signal transduction events (1, 2). These modules, such as SH2 domains (3), are small conserved domains that bind specific sequences in target proteins and recruit proteins into signaling complexes. Serine or threonine phosphorylation appears to regulate the formation of protein complexes (2) and acts as a signal to trigger ubiquitination and subsequent degradation of a wide range of regulatory proteins (4). With the exception of phosphoserine (pSer)- or phosphothreonine (pThr)-binding proteins 14-3-3 (5), small independent pSer- or pThr-binding modules reminiscent of SH2 domains have not been described. Similarly, it is not known whether phosphoproteins directly interact with ubiquitin-protein ligases (E3), enzymes that mediate substrate recognition in the ubiquitin-mediated pathway (6).

WW domains contain 38 to 40 amino acid

residues in a triple-stranded β sheet (7–10). These small modules are found in proteins that participate in cell signaling or regulation, including the peptidyl-prolyl isomerase (PPIase) Pin1 and the ubiquitin ligase Nedd4 (7–10). WW domains have been implicated in mediating protein-protein interactions by binding to Pro-rich motifs (10). However, bona fide Pro-rich motifs are not found in many potential WW domain targets, such as Nedd4 substrates (11) and Pin1-binding proteins (12–14). Pin1 is an essential regulator at mitotic entry that binds a defined subset of mitosis-specific phospho-

proteins, including the phosphatase Cdc25C, kinases Myt1 and Plk1, and the small guanosine 5'-triphosphate-binding protein Rab4 (12–14). Thus, the role of WW domains remains to be determined.

We examined whether WW domains might mediate protein-protein interactions by binding pSer or pThr. Glutathione S-transferase (GST)-fusion proteins containing Pin1, its NH₂-terminal WW domain (amino acids 1 to 54), or COOH-terminal PPIase domain (47 to 163) were incubated with extracts from interphase or mitotic HeLa cells. Bound proteins were detected by the monoclonal antibody MPM-2 that recognizes the overlapping subset of Pin1-binding proteins, or by antibodies to specific proteins (15). Although no specific binding was detected for the PPIase domain or control GST, WW domains of Pin1 and its yeast homolog Ess1 bound almost all of Pin1-binding proteins present in mitotic extracts (Fig. 1, A and B).

To test whether WW domain binding is phosphorylation-dependent and whether it is mediated by specific pSer or pThr residues in Pin1 target proteins, we analyzed binding to Cdc25C (16) because Pin1 interacts with Cdc25C just before entry into mitosis and regulates its activity (13). Both Pin1 and its WW domain bound the mitotically phosphorylated, but not the interphase phosphorylated, form of Cdc25C (Fig. 2A). Furthermore, they failed to bind Cdc25C if the mitotically phosphorylated Cdc25C was dephosphorylated (Fig. 2A). These results demonstrate a phosphorylation-dependent interaction between the WW domain and Cdc25C. Pin1 and its WW domain were found to bind two conserved pThr-Pro sites (Thr⁴⁸ and Thr⁶⁷) in Cdc25C, as identified by

Table 1. Binding constants of WW domains and peptides. The NH₂-terminus of peptides was labeled with fluorescein and purified by thin-layer chromatography. Various concentrations of GST-WW domains and control GST were incubated with the labeled peptides, and dissociation constants were measured by fluorescence anisotropy assay. Each value (in micromolar) represents the average of the three independent experiments. No binding was detected between GST and any peptides. NB, no binding detected.

WW domain	Peptide		Cdc25 peptide		Pro-rich peptide
	WFYpSPFLE	WFYSPFLE	EQLPtPVTDL	EQPLTPVTDL	IPGTPPPNYD
Pin1	1.0	NB	2.2	NB*	NB
Nedd4	10.0	NB	20.0	NB*	>40† (47–118‡)

*No binding detected by incubating the GST-WW domain with the peptide immobilized on a membrane, followed by immunoblotting analysis with antibody to GST (17). †An estimated K_d because binding did not reach the plateau even at 100 μ M WW domain. ‡Previously reported K_d 's for the interaction between the Yap WW domain and various Pro-rich peptides (9). Single-letter abbreviations for the amino acid residues are as follows: A, Ala; C, Cys; D, Asp; E, Glu; F, Phe; G, Gly; H, His; I, Ile; K, Lys; L, Leu; M, Met; N, Asn; P, Pro; Q, Gln; R, Arg; S, Ser; T, Thr; V, Val; W, Trp; and Y, Tyr.

Cancer Biology Program, Division of Hematology/Oncology, Department of Medicine, Beth Israel Deaconess Medical Center and Harvard Medical School, Boston, MA 02215, USA.

*These authors contributed equally to this work.

†To whom correspondence should be addressed. E-mail: klu@caregroup.harvard.edu